

# A Model for $\text{HCO}_3^-$ Accumulation and Photosynthesis in the Cyanobacterium *Synechococcus* sp.

## THEORETICAL PREDICTIONS AND EXPERIMENTAL OBSERVATIONS

Received for publication June 11, 1984 and in revised form October 9, 1984

MURRAY R. BADGER\*, MARY BASSETT, AND HUGH N. COMINS  
*Department of Environmental Biology, Research School of Biological Sciences, Australian National University, P.O. Box 475, Canberra, A.C.T. 2601 Australia*

### ABSTRACT

A simple model based on  $\text{HCO}_3^-$  transport has been developed to relate photosynthesis and inorganic carbon fluxes for the marine cyanobacterium, *Synechococcus* sp. Nægeli (strain RRIMP N1). Predicted relationships between inorganic carbon transport,  $\text{CO}_2$  fixation, internal carbonic anhydrase activity, and leakage of  $\text{CO}_2$  out of the cell, allow comparisons to be made with experimentally obtained data. Measurements of inorganic carbon fluxes and internal inorganic carbon pool sizes in these cells were made by monitoring time-courses of  $\text{CO}_2$  changes (using a mass spectrometer) during light/dark transients. At just saturating  $\text{CO}_2$  conditions, total inorganic carbon transport did not exceed net  $\text{CO}_2$  fixation by more than 30%. This indicates  $\text{CO}_2$  leakage similar to that estimated for  $\text{C}_4$  plants.

For this leakage rate, the model predicts the cell would need a conductance to  $\text{CO}_2$  of around  $10^{-5}$  centimeters per second. This is similar to estimates made for the same cells using inorganic carbon pool sizes and  $\text{CO}_2$  efflux measurements. The model predicts that carbonic anhydrase is necessary internally to allow a sufficiently fast rate of  $\text{CO}_2$  production to prevent a large accumulation of  $\text{HCO}_3^-$ . Intact cells show light stimulated carbonic anhydrase activity when assayed using  $^{18}\text{O}$ -labeled  $\text{CO}_2$  techniques. This is also supported by low but detectable levels of carbonic anhydrase activity in cell extracts, sufficient to meet the requirements of the model.

Photosynthesis and  $\text{C}_i$  usage in cyanobacteria has been shown to function through the combined operation of RuBP carboxylase activity and a  $\text{CO}_2$  concentrating mechanism (7, 9). At alkaline pH values, favored by most cyanobacteria, it is apparent that the bicarbonate ion is the major source of  $\text{C}_i$  for the concentrating mechanism (2, 10) although it appears that both  $\text{CO}_2$  and  $\text{HCO}_3^-$  may be able to act as substrate for this accumulation (2). The mechanism responsible for  $\text{C}_i$  uptake is unclear but it is most frequently suggested to involve a  $\text{HCO}_3^-$  transport system, possibly a primary electrogenic pump (8).

Gas exchange measurements with *Synechococcus* sp. have shown that general characteristics of  $\text{CO}_2$  uptake and efflux are consistent with a model of photosynthesis in which  $\text{HCO}_3^-$  is accumulated within the cell (2). During steady state photosynthesis,  $\text{CO}_2$  is constantly effluxing from the cell, being derived presumably from a concentrated internal  $\text{C}_i$  pool. It is unclear,

however, with *Synechococcus* and other cyanobacteria, what the balance is between transport of  $\text{C}_i$  into the cell,  $\text{CO}_2$ -fixation, and the leakiness of the cell to  $\text{CO}_2$  efflux. The role of CA in the operation of the  $\text{CO}_2$  concentrating mechanism is also uncertain.

An attempt is made here to develop a simple quantitative model of photosynthesis in *Synechococcus* sp., deriving relationships between  $\text{C}_i$  carbon transport,  $\text{CO}_2$ -fixation, leakage to  $\text{CO}_2$ , and CA activity. This model is then compared with experimentally obtained estimates of these parameters in air-adapted cells, with good correlation being found.

### MATERIALS AND METHODS

The unicellular marine cyanobacterium used in these studies is classified according to Rippka *et al.* (12) as *Synechococcus* sp. Nægeli (strain RRIMP N1) and is an oval rod of dimensions  $1.5 \times 3 \mu\text{m}$ . It is considered to belong to the same group as *Agmenellum quadruplication* and *Coccochloris elabens* (11). [ $^3\text{H}$ ]inulin and  $^3\text{H}_2\text{O}$  were obtained from Amersham (UK). [ $^{18}\text{O}$ ]H $_2\text{O}$  was from Norsk Hydro (Oslo, Norway).

**Growth of *Synechococcus*.** The cells were grown to late log phase in 300-ml batches contained in conical flasks. Growth medium was a 0.2  $\mu\text{m}$  filter-sterilized seawater medium based on the f medium of Guillard and Ryther (5), and buffered at pH 8.2 with 50 mM Bicine. Cultures were shaken in a temperature-controlled water bath (30°C) and bubbled with humidified air. Light (400  $\mu\text{mol m}^{-2} \text{s}^{-1}$  photon flux density, at the surface of the culture vessels) was provided by a Hg vapor lamp suspended over the bath.

**Preparation and Assay of Cells.** Cells were harvested by centrifugation at 5000g for 10 min, and resuspended in 2 to 3 ml of  $\text{CO}_2$ -free culture media. The cells were stored in the dark on the bench and slowly bubbled with  $\text{CO}_2$ -free air prior to their use in all experiments. All assays were performed in seawater medium at pH 8.2 and 30°C.

**Cell Parameter Measurements.** The internal volume per cell was estimated from silicone oil centrifugation experiments, measuring the [ $^3\text{H}$ ]inulin impermeable space of the cells (see Kaplan *et al.* [7]). This was combined with haemocytometer estimates of cell numbers to give an average value of  $2.3 \pm 0.4 \times 10^{-2} \text{cm}^3 \cdot \text{cell}^{-1}$  ( $n = 8$ ). Assuming the cells were spherical, the surface area of a cell with this volume is  $8.4 \pm 0.7 \times 10^{-8} \text{cm}^2 \cdot \text{cell}^{-1}$ . Chl *a* was estimated according to Wintermans and de Mots (14) and an average value of  $0.33 \pm 0.05 \mu\text{g Chl } a \cdot \text{cell}^{-1}$  ( $n = 8$ ) was calculated.

**Photosynthetic  $\text{O}_2$  Evolution.** This was measured in an  $\text{O}_2$  electrode chamber (Hansatech, England).

**Mass Spectrometric Studies.** Monitoring of dissolved  $\text{CO}_2$  species in aqueous algal suspensions was achieved through the

\* Abbreviations:  $\text{C}_i$ , inorganic carbon ( $\text{CO}_2 + \text{HCO}_3^- + \text{CO}_3^{2-}$ ); CA, carbonic anhydrase.

use of a stirred glass cuvette aqueous inlet system, attached to a mass spectrometer as previously described (2). Algal suspensions were illuminated ( $400 \mu\text{mol photons m}^{-2} \cdot \text{s}^{-1}$ ) with a quartz halogen projector lamp.

Calibration of the instrument with  $\text{CO}_2$  was achieved by bubbling air of a known  $\text{CO}_2$  partial pressure through the liquid in the cuvette and calculating dissolved  $\text{CO}_2$  using the Henry constant. The distribution between  $\text{HCO}_3^-$  and  $\text{CO}_2$  was calculated by injecting known amounts of  $\text{NaHCO}_3$  into the cuvette and measuring the appearance of  $\text{CO}_2$ . This measured distribution was used to calculate the total  $\text{C}_i$  uptake or evolution represented by a change in  $\text{CO}_2$ .

Uniformly labeled  $[^{18}\text{O}]\text{NaHCO}_3$  was prepared by dissolving  $\text{NaHCO}_3$  in  $[^{18}\text{O}]\text{H}_2\text{O}$  (99% enrichment), and allowing 3 d for the label in the  $\text{H}_2\text{O}$  and  $\text{HCO}_3^-$  to reach isotopic equilibrium. The mixture was then frozen and freeze-dried to recover the solid salt.

**Carbonic Anhydrase Measurements.** Cells were harvested by centrifugation as described above. The cell pellet was resuspended in extraction buffer (100 mM Bicine [pH 8.0], 1 mM EDTA, 5 mM DTT), and ruptured by passing them twice through a French pressure cell (10,000 p.s.i.). The homogenate was spun at  $15,000g$  for 20 min and the supernatant retained for assay. The pellet showed no detectable CA activity (data not shown). Assays were performed in a glass water-jacketed cuvette ( $0^\circ\text{C}$ ) and the reaction monitored with a glass pH electrode. The assay was 3 ml reaction buffer (20 mM Veronal [pH 8.2], 5 mM DTT), 0.3 ml of extract or extraction buffer, and 1.5 ml of  $\text{CO}_2$  saturated water ( $0^\circ\text{C}$ ). The time for the pH drop between 7.9 and 6.9 was monitored.

## RESULTS

**The Model. Assumptions.** A simple model of photosynthesis can be constructed if one considers *Synechococcus* as a single spherical compartment, into which  $\text{C}_i$  is actively accumulated, fixed as  $\text{CO}_2$  into glycerate 3-P and continually effluxing as  $\text{CO}_2$  (Fig. 1). In trying to quantitatively define various parts of this system the following assumptions must be made.

(a) How is  $\text{C}_i$  entering the cell? The simplest assumption is that it is entering as  $\text{HCO}_3^-$  (—). It is, however, possible considering evidence from active species experiments with *Synechococcus* (2) to suggest that a number of other possibilities exist (...): (i) free  $\text{CO}_2$  may be actively taken up directly and enter the cells as  $\text{CO}_2$  OR  $\text{HCO}_3^-$  (ii)  $\text{HCO}_3^-$  may be converted to  $\text{CO}_2$  externally and enter as  $\text{CO}_2$ .

Considering the evidence available, it is reasonable to suggest that in whatever form  $\text{C}_i$  is taken up, it enters the cell as  $\text{HCO}_3^-$ .

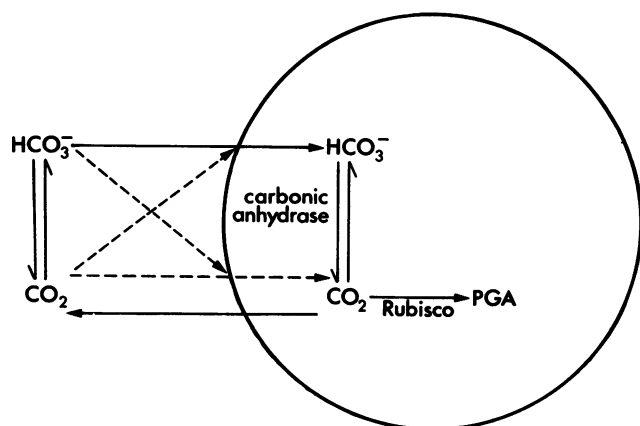


FIG. 1. Schematic model showing possible fluxes of  $\text{CO}_2$  and  $\text{HCO}_3^-$  into and out of a *Synechococcus* cell.

This stems from consideration of: (i) the efflux of  $\text{CO}_2$  from *Synechococcus* cells following illumination (2; Fig. 4, top) can only be explained if  $\text{HCO}_3^-$  is accumulated from the external medium at a rate in excess of net  $\text{CO}_2$  fixation; (ii) it is energetically more feasible to construct models for active  $\text{HCO}_3^-$  uptake, than for  $\text{CO}_2$  accumulation, and experiments measuring hyperpolarization of cyanobacterial cells upon addition of external  $\text{HCO}_3^-$  suggest a primary electrogenic  $\text{HCO}_3^-$  pump (8).

Thus it will be assumed at present that  $\text{C}_i$  enters the cell as  $\text{HCO}_3^-$ , and that this is largely derived from external  $\text{HCO}_3^-$ .

(b) Once  $\text{HCO}_3^-$  is inside the cell, then it can only be fixed by RuBP carboxylase upon conversion to  $\text{CO}_2$ . In this step CA is most likely to play a role. Hence it will be considered low varying amounts of CA may affect the size of the internal  $\text{HCO}_3^-$  pool necessary to support  $\text{CO}_2$  fixation by RuBP carboxylase.

(c)  $\text{C}_i$  is largely leaving the cell, under steady state conditions, as  $\text{CO}_2$ , by passive diffusion determined by the concentration gradient across the membrane and the conductance to  $\text{CO}_2$ . This neglects the possibility that  $\text{C}_i$  species may be effluxing via reversal of the  $\text{C}_i$  transport system.

**Balance between Bicarbonate Transport,  $\text{CO}_2$  Fixation, and Cell Conductance to  $\text{CO}_2$ .** The relationship between  $\text{HCO}_3^-$  transport into the cell ( $V_i$ ),  $\text{CO}_2$  fixation ( $V_c$ ), and conductance of the cell to  $\text{CO}_2$  efflux ( $g$ ) may be derived at the point where  $\text{CO}_2$  fixation is just saturated with external  $\text{C}_i$ . At this point it can be assumed that  $\text{CO}_2$  inside is saturating for RuBP carboxylase ( $1000 \mu\text{M}$  or  $5 K_m(\text{CO}_2)$  [1]). Given that  $\text{CO}_2$  is small externally compared to this internal level, the  $\text{CO}_2$  gradient will be  $1000 \mu\text{M}$ . Under steady state conditions,

$$V_i = V_c + g \times \Delta C \times A \times 10^{-3} \quad (1)$$

and

$$g = \frac{V_i - V_c}{\Delta C \times A} \times 10^3 \quad (2)$$

where  $V_i$  is in  $\text{mol cell}^{-1} \text{s}^{-1}$ ,  $V_c$  is  $\text{mol cell}^{-1} \cdot \text{s}^{-1}$ ,  $\Delta C = 10^{-3} \text{ mol l}^{-1}$ ,  $A$  = surface area per cell ( $\text{cm}^2 \text{ cell}^{-1}$ ), and  $g$  = cell  $\text{CO}_2$  conductance in ( $\text{cm s}^{-1}$ ).

Cell size parameters for *Synechococcus* are given in "Materials and Methods". Using these numbers combined with measured  $\text{CO}_2$  fixation rates, this model can be quantified for a range of conditions. Figure 2 presents the relationship between  $V_c$ ,  $V_i$ , and  $g$  for two extremes of  $\text{CO}_2$  fixation ( $18\text{--}55 \times 10^{-19} \text{ mol cell}^{-1} \text{s}^{-1}$ ). Cell conductance to  $\text{CO}_2$  diffusion out ( $g$ ) is allowed to vary from  $10^{-3}$ – $10^{-6} \text{ cm s}^{-1}$ , and the ratio of  $V_i/V_c$  is calculated over this range (assuming internal  $\text{CO}_2$  to be  $1000 \mu\text{M}$ ). Also presented in this same figure is the  $\text{O}_2$  gradient, which would be expected to exist between the cell and the medium, assuming net  $\text{O}_2$  production is equal to  $V_c$ , and  $\text{O}_2$  conductance is the same as  $\text{CO}_2$  conductance.

At cell conductances above  $10^{-4} \text{ cm s}^{-1}$ , the ratio of  $V_i$  to  $V_c$  increases markedly. Depending on the energetic cost of transport, it would seem inefficient for the cell to operate in this region. Indeed, to limit  $V_i$  to  $< 2 V_c$ ,  $g$  would need to be about  $10^{-5} \text{ cm s}^{-1}$ . A difficulty that the cell would encounter in achieving a suitable balance of  $V_i$  to  $V_c$  is the buildup of  $\text{O}_2$  within the cell. The  $\text{O}_2$  gradient rapidly increases to levels in excess of one atmosphere partial pressure with  $g$  less than  $5 \times 10^{-5} \text{ cm s}^{-1}$ , depending on the absolute value of  $V_c$ .

**Carbonic Anhydrase Levels.** Internal CA will affect the rates of  $\text{CO}_2$  hydration and  $\text{HCO}_3^-$  dehydration within the cell. Under steady state equilibrium conditions the net rate of  $\text{CO}_2$  production within the cell will be given by  $(k_1 [\text{HCO}_3^-] - k_2 [\text{CO}_2] \cdot \text{vol})$ , where  $k_1 = 10^{(-\text{pH})} \times 10.47 \times 10^4 \text{ s}^{-1}$ ,  $k_2 = 3.72 \times 10^{-2} \text{ s}^{-1}$  (11), and vol is the internal cell volume ( $l \cdot \text{cell}^{-1}$ ). Given that this will equal the rate of  $\text{HCO}_3^-$  transport into the cell ( $V_i$ ), given by equation 1, then the internal  $[\text{HCO}_3^-]$  which will accumulate

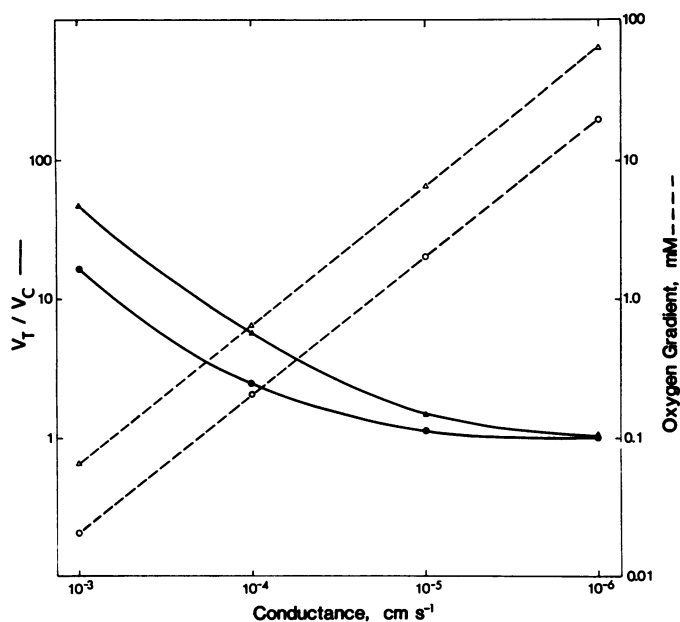


FIG. 2. Possible relationship between the ratio of C<sub>i</sub> transport ( $V_t$ ) to carbon fixation ( $V_c$ ) given various cell conductances to CO<sub>2</sub>. Data are derived from model calculation as described in text, for two  $V_c$  values ( $18 \text{ [}\bullet\text{]} \text{ and } 55 \text{ [}\blacktriangle\text{]} \times 10^{-19} \text{ mol cell}^{-1} \cdot \text{s}^{-1}$ ). Also shown is the oxygen gradient (---) which would develop between cell and bulk medium for each of these conditions.

in order to support CO<sub>2</sub> saturated rates of photosynthesis may be calculated. Carbonic anhydrase is simulated by multiplying  $k_1$  and  $k_2$  by some constant representing the relative rate of interconversion of CO<sub>2</sub> and HCO<sub>3</sub><sup>-</sup> relative to the uncatalyzed condition. Internal [HCO<sub>3</sub><sup>-</sup>] has been calculated allowing cell CO<sub>2</sub> conductance ( $g$ ) and CA levels to vary (Fig. 3).

Without CA inside the cell, then HCO<sub>3</sub><sup>-</sup> levels would have to build up to high levels in order to support CO<sub>2</sub>-saturated photosynthesis. The level decreases as conductance ( $g$ ) decreases, but asymptotically approaches about 2.0 M internal HCO<sub>3</sub><sup>-</sup>. Increasing the interconversion rate from 1- to 1000-fold obviously results in decreased internal HCO<sub>3</sub><sup>-</sup>. Measured internal C<sub>i</sub> pools in *Synechococcus* and other cyanobacteria at CO<sub>2</sub> saturation, appear to be in the region of 30 to 60 mM (2, 7, 9). For cell conductances of  $10^{-4}$  to  $10^{-5} \text{ cm s}^{-1}$ , these levels are achieved in the model for an increase of interconversion of 100- to 1000-fold. Thus, there is an obvious need in this model for CA to allow the maintenance of reasonable HCO<sub>3</sub><sup>-</sup> levels inside the cell. These calculations assume that the internal pH is 8.0. Obviously, the magnitude of the HCO<sub>3</sub><sup>-</sup> pool necessary to sustain a particular rate of conversion to CO<sub>2</sub> will depend on the true pH. If the pH was lower than this, then calculated HCO<sub>3</sub><sup>-</sup> would be lower.

**Measurement of Internal CA. *In Vitro Assay.*** A problem with assigning a role for CA in photosynthesis models of cyanobacteria, is that conflicting evidence exists as to the presence or absence of CA in these cells. Ingle and Coleman (6) measured low but detectable levels of CA in low CO<sub>2</sub>-grown *Coccochloris peniocystis* which declined when cells were adapted to high CO<sub>2</sub>. More recently, studies with *Anabaena variabilis* (7) have failed to detect any activity in low CO<sub>2</sub>-grown cells, even though the CA inhibitor, ethoxzolamide, affected the affinity of photosynthesis for C<sub>i</sub>.

Measurement of CA activity in low CO<sub>2</sub>-grown cells of *Synechococcus* sp. shows low but detectable presence of a factor speeding up the interconversion of CO<sub>2</sub> and HCO<sub>3</sub><sup>-</sup>. In two experiments this activity was measured as 43 and 52 WA

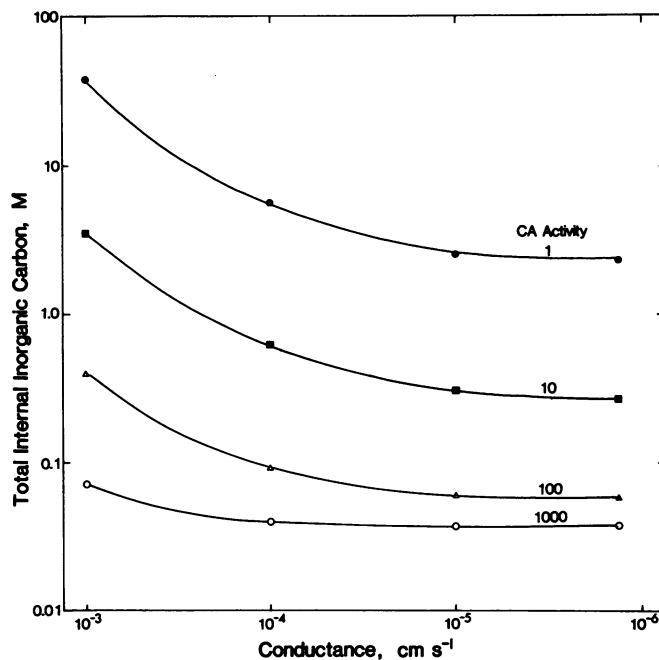


FIG. 3. Effect of various CA levels on the predicted internal HCO<sub>3</sub><sup>-</sup> levels developed within the cell, for varying values of cell conductance to CO<sub>2</sub>. Carbon fixation is assumed to be  $55 \times 10^{-19} \text{ mol cell}^{-1} \cdot \text{s}^{-1}$  and CA levels are expressed as the speed of interconversion of C<sub>i</sub> species, relative to the uncatalyzed condition. Calculations are described in the text.

units  $\cdot \text{mg}^{-1}$  Chl *a*. Taking the average Chl *a* and volume per cell (see "Materials and Methods"), this activity can be confined to the internal cell volume and would result in an increase in the rate of interconversion between CO<sub>2</sub> and HCO<sub>3</sub><sup>-</sup> of 350- and 290-fold, respectively. This increased interconversion can be directly compared to the effect of different levels of CA on the operation of the photosynthetic model presented in Figure 3. Activity levels fall in the region sufficient to promote a 100- to 1000-fold increase in internal interconversion rate.

***In Vivo Assay.*** A technique for detecting CA within photosynthesizing cells is by the use of <sup>18</sup>O labeled CO<sub>2</sub> and HCO<sub>3</sub><sup>-</sup>. In normal seawater medium at pH 8.0 and above, the rate of exchange of <sup>18</sup>O out of C<sub>i</sub> species into water is relatively slow (13), taking of the order of 1 h or more to reach isotopic equilibrium. This exchange can be measured by monitoring the doubly, singly, and unlabeled species of CO<sub>2</sub> in solution, mass spectrometrically. On a background of slow exchange then, cells can be injected into media and their effects on the overall rate of interconversion of CO<sub>2</sub> and HCO<sub>3</sub><sup>-</sup> can be assessed.

If CA is located within the cells, and both CO<sub>2</sub> and HCO<sub>3</sub><sup>-</sup> are freely permeable into this space, then adding cells will increase the rate of interconversion detected externally. If, however, only CO<sub>2</sub> is permeable, then little effect of adding cells would be expected. If HCO<sub>3</sub><sup>-</sup> access to the internal CA is mediated by a light-dependent pump, then very different results may be expected. In this case, when the light is switched on HCO<sub>3</sub><sup>-</sup> will accumulate inside the cells, where it will rapidly exchange with CO<sub>2</sub> and H<sub>2</sub>O and lose <sup>18</sup>O label. The CO<sub>2</sub> which diffuses back from the cell will be largely unlabeled with respect to <sup>18</sup>O. An experiment testing the effect of cells on the exchange of <sup>18</sup>O from CO<sub>2</sub> species in solution is shown in Figure 4.

In the absence of cells a steady state rate of exchange of <sup>18</sup>O between isotopic species of CO<sub>2</sub> and HCO<sub>3</sub><sup>-</sup> is established. With the levels of the various species used here it is evident that the decrease in doubly labeled CO<sub>2</sub> (Fig. 4, 48) is accompanied by an increase in singly (Fig. 4, 46) and unlabeled CO<sub>2</sub> (Fig. 4, 44).

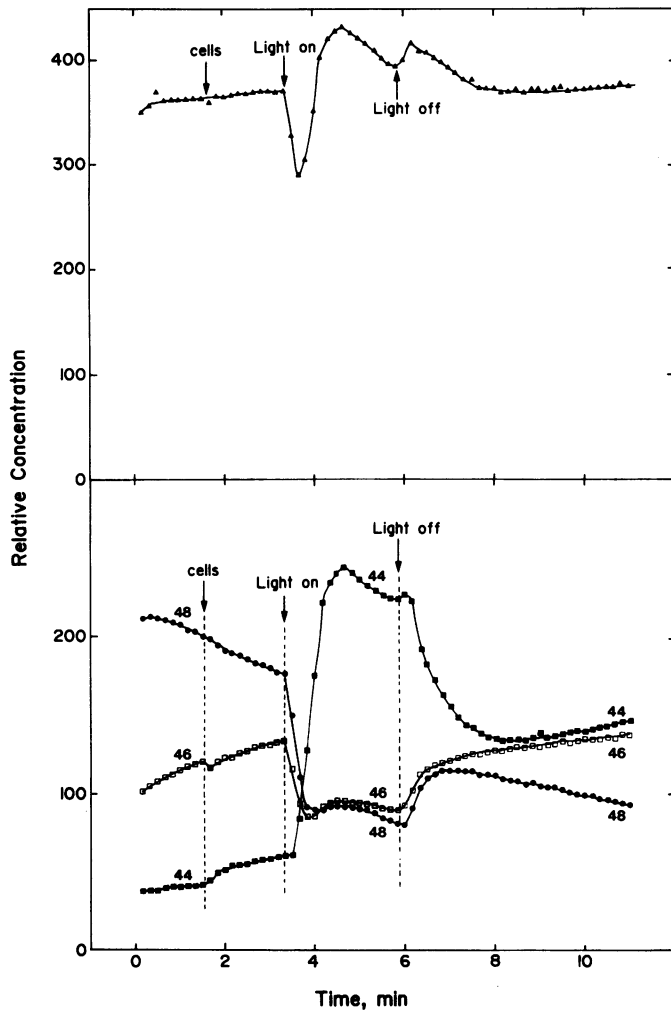


FIG. 4. Change in the relative concentration of [ $^{18}\text{O}$ ]  $\text{CO}_2$  species in solution during a time course. The time course involved addition of cells ( $8 \mu\text{g Chl}\cdot\text{ml}^{-1}$ ) in the dark, switching on the light, and then darkening. The change in total  $\text{CO}_2$  species is shown in the upper box, while changes in the three individual species are shown below. The total concentration of  $\text{C}_i$  species was initially  $0.5 \text{ mM}$ .

Addition of cells (in the dark) to this medium caused little change in the exchange rate, apart from adding a small amount of unlabeled  $\text{CO}_2$  with the addition of the cells. A dramatic effect, however, is seen when the light is switched on. There is an uptake of doubly and singly labeled  $\text{CO}_2$  species within the first 30 s, followed by a slight increase, which eventually settles down to a steady decrease in both species. Unlabeled  $\text{CO}_2$ , however, shows no initial uptake in the first 30 s, but instead shows a massive increase over the period that slight increases are seen in the other two species. There is a peak in unlabeled  $\text{CO}_2$  level, followed by a decline over the rest of the light period. When the light is switched off there is an increase in the level of labeled species until an exchange pattern similar to that before the light is switched on is reached, with 48 decreasing and 46 increasing. Unlabeled  $\text{CO}_2$ , however, shows a slight increase followed by a dramatic decrease over the following 3 min until a steady state rate of increase is established, similar to that occurring before the light is switched off.

In all, the events seen here are consistent with cells having a light dependent  $\text{HCO}_3^-$  pump which accumulates  $\text{HCO}_3^-$  in a region of rapid exchange between  $\text{CO}_2$  and  $\text{HCO}_3^-$ . The unlabeled  $\text{CO}_2$  evolution would be a result of exchange of label within

the cell and diffusion of unlabeled  $\text{CO}_2$  out of the cell. The slight increase in labeled species following initial uptake in the light could be the result of less than complete exchange of  $^{18}\text{O}$  out of  $\text{CO}_2$  within the cell, thus leading to some labeled  $\text{CO}_2$  evolution, or a decline in  $\text{CO}_2$  uptake following the initial transient after turning on the light. Initial uptake of  $\text{CO}_2$  species is presumably due to some direct  $\text{CO}_2$  uptake process as has been seen previously (2). An increase in labeled species following turning off the light could be due to labeled  $\text{CO}_2$  being evolved from the cell and/or a simple reequilibration of species in solution following the cessation of direct  $\text{CO}_2$  uptake. The decline in unlabeled  $\text{CO}_2$  is consistent with a gradual decline in the rate of evolution of unlabeled  $\text{CO}_2$  into the medium as the internal pool of  $\text{C}_i$  is depleted.

This experiment shows there is strong evidence for implicating the existence of a light-dependent  $\text{HCO}_3^-$  influx mechanism, together with rapid equilibration of  $\text{CO}_2$  and  $\text{HCO}_3^-$  within the cell.

**Effects of Ethoxzolamide.** The CA inhibitor, ethoxzolamide, has been shown to have a dramatic effect on photosynthesis in air-adapted green algae. It decreases their affinity for external  $\text{C}_i$  without altering  $\text{CO}_2$  saturated photosynthesis, thus making them more like high  $\text{CO}_2$  grown cells (3). As the two previous *in vitro* and *in vivo* experiments suggest that CA activity does exist in air-adapted cells of *Synechococcus* sp., an effect of ethoxzolamide might be expected on these cells. The response of photosynthetic  $\text{O}_2$  evolution to  $\text{C}_i$  in these cells has proven to be unaffected by ethoxzolamide levels from 10 to  $100 \mu\text{M}$  (data not shown). This result was somewhat unexpected considering the earlier data, and the previously reported inhibition of  $\text{CO}_2$ -limited photosynthesis in the cyanobacterium *Anabaena variabilis* (7).

**Measurement of  $\text{C}_i$  Uptake, Efflux, and Pool Sizes.** To obtain a quantitative understanding of the performance of the cell in relation to the proposed photosynthesis model, measurement of parameters of  $\text{C}_i$  uptake, efflux, and pool sizes, together with photosynthesis is necessary.

Measurement of these parameters can be achieved by monitoring the uptake and efflux of  $\text{CO}_2$  from cells under appropriate conditions. Cells in seawater medium, and in the absence of any added external CA, show a pattern of  $\text{CO}_2$  uptake following illumination and darkness, which is similar to the change in total  $\text{CO}_2$  species seen in Figure 4. Under these conditions,  $\text{CO}_2$  and  $\text{HCO}_3^-$  are not in rapid equilibrium, so changes in  $\text{CO}_2$  are somewhat independent of changes in  $\text{HCO}_3^-$ . If CA is added then a different time-course is obtained (Fig. 5). Under these conditions, the  $\text{CO}_2$  signal is representative of the total  $\text{C}_i$  species.

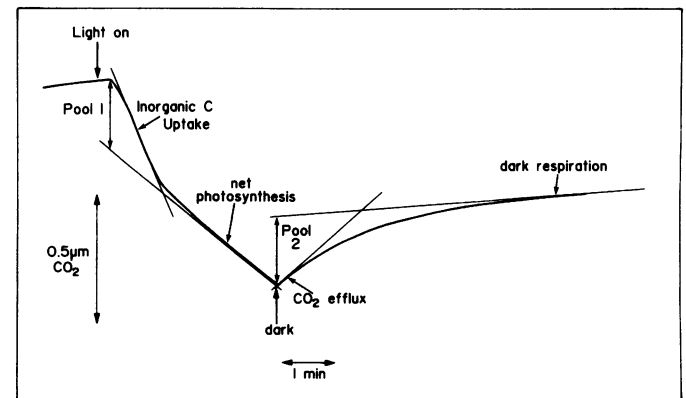


FIG. 5. Time course of changes in  $\text{CO}_2$  concentration in an algal suspension ( $1.5 \mu\text{g Chl}\cdot\text{ml}^{-1}$ ) showing effects of light and dark transients. CA at  $0.2 \text{ mg}\cdot\text{ml}^{-1}$  was included. Initial  $\text{CO}_2$  was  $2.1 \mu\text{M}$ . The rationale for the drawing of the shown tangents and pool 1 and pool 2 regions are described in the text.

The time-course has three distinct phases. Following illumination, there is a 15- to 20-s delay in CO<sub>2</sub> uptake, followed by a linear phase of CO<sub>2</sub> uptake for the next 30 to 90 s, depending on the C<sub>i</sub> level. This uptake phase slows down and is followed by a slower and longer second period of linear CO<sub>2</sub> uptake. Following darkness, CO<sub>2</sub> uptake is replaced by CO<sub>2</sub> evolution, which declines over a 4- to 6-min period to the level of dark respiration. The first CO<sub>2</sub> uptake phase can be attributed to the uptake of C<sub>i</sub> into a pool within the cell. As this pool is filled, this net uptake will be replaced by a steady rate of net CO<sub>2</sub> fixation, as seen in the second phase. When the light is turned off, presumably C<sub>i</sub> uptake and CO<sub>2</sub> fixation is stopped and the inorganic carbon pool will be released to the medium. The initial rate of C<sub>i</sub> release in the dark most probably represents the CO<sub>2</sub> evolution occurring continuously in the light prior to darkness.

Thus, the following measurements may be made from such a time course. (a) The initial slope of the first phase of CO<sub>2</sub> uptake can be taken as an estimate of C<sub>i</sub> transport into the cell. (b) The slope of the second region of uptake can be taken as a measure of steady state net CO<sub>2</sub> fixation. (c) The initial slope of the efflux in the dark, minus dark respiratory CO<sub>2</sub> output, can be used as an estimate of C<sub>i</sub> leakage from the cell just before the light was turned off. (d) Steady state C<sub>i</sub> uptake in the light just prior to darkness can be estimated as net CO<sub>2</sub> fixation plus C<sub>i</sub> efflux. (e) Internal C<sub>i</sub> pool sizes can be estimated from two regions of the time-course: (i) If the net CO<sub>2</sub> fixation slope is extrapolated back to the light-on time, then the drop in CO<sub>2</sub> from light-on to the extrapolated CO<sub>2</sub> fixation, gives an estimate of the amount of C<sub>i</sub> sequestered by the cell (pool 1). (ii) Conversely, if dark respiration is extrapolated back to the light-off time, then the distance pool 2 gives an estimate of the C<sub>i</sub> released into the medium by the cell, following darkness.

If both these pools are partitioned within the estimated cell volumes, then the concentration of C<sub>i</sub> within the cell can be calculated.

Experiments were conducted in which air-grown cells of *Synechococcus* were exposed to varying C<sub>i</sub> concentrations and the parameters described above in dark-light-dark time courses measured. As a result of the absolute sensitivity of the CO<sub>2</sub> measurement and the high affinity of the cells for CO<sub>2</sub>, these experiments could only be conducted at CO<sub>2</sub> concentrations at or above saturating for photosynthesis. Once saturating levels were reached, the cells used up most of the inorganic carbon before a complete time course could be achieved.

Estimates of four flux parameters at different external CO<sub>2</sub> concentrations are given in Figure 6. These are net CO<sub>2</sub> fixation, C<sub>i</sub> evolution and the two estimates of gross C<sub>i</sub> uptake (*i.e.* initial uptake and C<sub>i</sub> evolution + net CO<sub>2</sub> fixation). At CO<sub>2</sub> levels which are just saturating for net CO<sub>2</sub> fixation, total C<sub>i</sub> uptake by either estimate exceeds net fixation by about 30%. As CO<sub>2</sub> increases above this level inorganic carbon uptake continues to increase, despite the saturation of photosynthetic CO<sub>2</sub> fixation. Both estimates saturate at around 1.5 μM CO<sub>2</sub> at levels which are some 55 to 100% in excess of CO<sub>2</sub> fixation. Estimates of total C<sub>i</sub> uptake are higher for the initial uptake parameter than for evolution plus net uptake by about 40%; however, both show the same general response to external CO<sub>2</sub>.

The release of C<sub>i</sub> in the dark period has been assumed here to represent the leakage rate occurring in the light prior to darkness. It is possible, however, that several changes occurring in the dark may make this invalid. Transient changes leading to depolarization of the plasmalemma and decreased internal pH may lead to an increased rate of C<sub>i</sub> release relative to the light. Similarly, if significant leakage is occurring via a reversal of the C<sub>i</sub> transport system, then a decrease in energy supply in the dark may alter the efflux via this route. The similarity of estimates of leakage from both the initial C<sub>i</sub> uptake in the light and its release in the

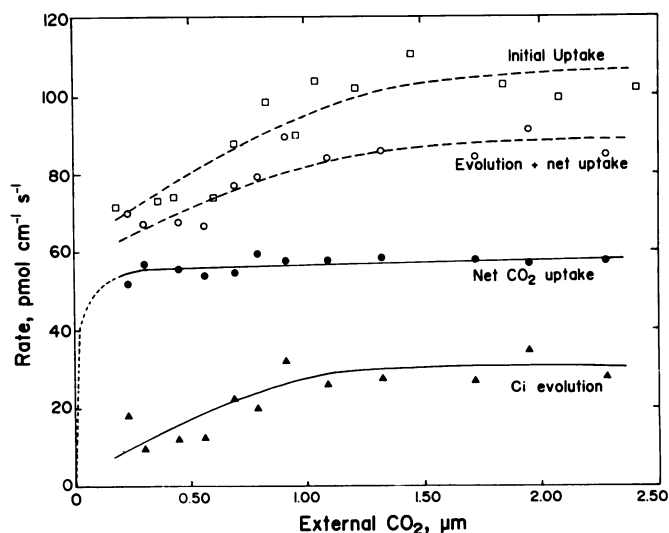


FIG. 6. Values for net CO<sub>2</sub> fixation, total C<sub>i</sub> uptake and C<sub>i</sub> evolution at varying external CO<sub>2</sub> in *Synechococcus* sp., obtained from light/dark time courses similar to those shown in Figure 5. Calculation of the data is described in the text. All data were collected for a single set of cells at a concentration of 0.8 μg Chl·ml<sup>-1</sup>. Different initial CO<sub>2</sub> concentrations were achieved by both varying the amount of added NaHCO<sub>3</sub> and also by performing several time courses on the same cell suspension, allowing the cells to deplete the medium of CO<sub>2</sub>. The cell parameters given in "Materials and Methods" were used to express the flux rates on a cm<sup>-2</sup> cell surface basis.

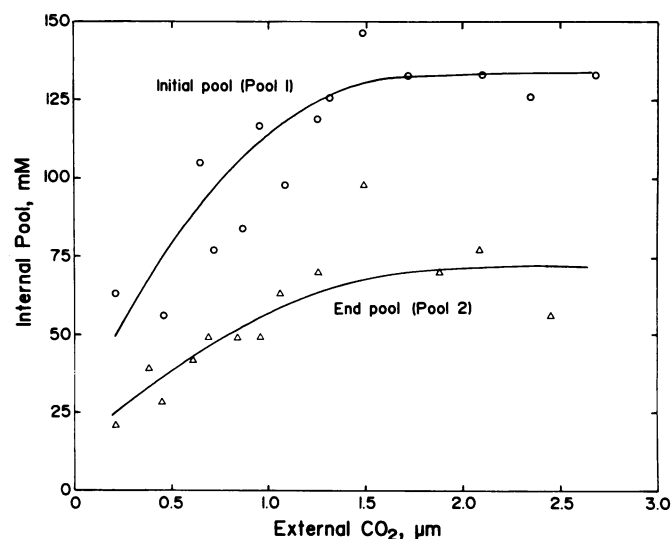


FIG. 7. The response of internal C<sub>i</sub> pool to external CO<sub>2</sub> in *Synechococcus* sp. Two pools (pool 1 and pool 2) are estimated from the data in Figure 6 as described in the text and in Figure 5.

dark indicates that such considerations may not be of great significance.

The internal C<sub>i</sub> pools (pool 1 and pool 2) calculated from these experiments are given in Figure 7. The initial pool 1 estimates prove to be some 100% higher than the end pool 2 values. At just saturating external CO<sub>2</sub>, internal (C<sub>i</sub>) is estimated at around 50 mM from pool 1 and 25 mM for pool 2. Both pools respond to increasing external CO<sub>2</sub> in a similar fashion and saturate at around 1.5 μM CO<sub>2</sub>. This agrees well with the response of total C<sub>i</sub> uptake which, ultimately, these pools are derived from. Significantly, the variation in the size of the pools are correlated with the total C<sub>i</sub> uptake values measured at the beginning and

end of the time course. Rather than being an artefact of measurement,  $C_i$  uptake may indeed be initially faster in the absence of  $CO_2$  fixation than at the end of the light period, and consequently the steady state internal pool sizes are larger at the beginning than the end of this period.

From the end pool and initial  $C_i$  efflux measurements, it is possible to make estimates of the cell conductance to  $CO_2$ . This assumes (a) the cell volume and surface dimensions given in "Materials and Methods"; (b) that  $CO_2$  is the major species effluxing; (c) that  $CO_2$  and  $HCO_3^-$  are in rapid equilibrium internally, and hence that the actual internal concentration of  $CO_2$  can be derived from the pool sizes and an estimated internal pH, using the  $pK_1$  of  $H_2CO_3$  (6.29). These conductance estimates, calculated for three assumed internal pH values (pH 7.5, 8.0, and 8.5), range from  $6.07 \pm 0.34 \times 10^{-6}$  at pH 7.5 to  $5.72 \pm 0.32 \times 10^{-4}$  at pH 8.5.

### DISCUSSION

The technique of monitoring  $CO_2$  (in the presence of CA) in solution during light/dark time courses, has helped quantify the steady state fluxes of  $C_i$  in photosynthesizing cells of *Synechococcus*. At levels of external  $C_i$  which are just saturating for photosynthesis, total  $C_i$  uptake is only about 30% higher than net  $CO_2$  fixation. This means that of the  $C_i$  being taken up and concentrated by the cell, only about 30% is leaking out into the external medium. This leakage becomes higher as  $C_i$  increases above levels which are saturating for fixation. This is due to a continuing response of the uptake system to increasing  $C_i$ , while fixation remains constant. The level of 30% leakage indicates that the system is relatively tight in terms of coupling uptake to  $CO_2$  fixation. Similar leakiness has been estimated for the higher plant  $C_4$   $CO_2$  concentrating system (4).

Internal pool size estimates from these experiments are in the range of values estimated in cyanobacteria, using silicone oil-centrifugation techniques. In these studies, pool sizes of 15 to 50  $\mu M$  for saturating external  $C_i$  have been obtained (2, 7, 9). The observation that the initial pool estimate is considerably higher than the pool estimated after a period of steady state photosynthesis may be related to changes in the rate of  $C_i$  uptake and  $CO_2$  fixation during the time course. Initially, in the absence of significant  $CO_2$  fixation and competition for energy, transport will probably be high. This, coupled to reduced  $CO_2$  fixation, would lead to high internal pools. This balance would adjust as competition for energy changed and  $CO_2$  fixation increased. The pool size at the end of the time course is probably more relevant in considering the pool sizes which are necessary to support photosynthesis. Likewise, the uptake measurements estimated at this time are also most pertinent to assessing the balance between transport and fixation during steady state photosynthesis. It is significant that transport estimates are higher in the initial period than after steady state photosynthesis. This would support the interpretation of why pool sizes vary as discussed above.

Carbonic anhydrase activity is readily detected in intact cells (Fig. 4) using the  $^{18}O$  labeled  $CO_2$  technique. This, coupled to small but detectable levels of assayable activity in broken cells, suggests that it may be reasonable to assume that  $HCO_3^-$  and  $CO_2$  may be near chemical equilibrium within the cell. This finding is in contrast to previous interpretations that  $C_i$  species may be far from chemical equilibrium due to an absence of CA (7).

Calculation of cell conductance values for passive  $CO_2$  efflux shows that the cell may have interesting properties with regard to gas diffusion. At reasonable estimates of internal pH (pH 7.5–8), it would appear that conductance values of around  $10^{-5}$   $cm^2 s^{-1}$  are necessary to explain the leakage rates of  $CO_2$  that are measured (Fig. 6). This value is extremely low compared to estimates of other biological membrane systems; however, it is

similar to an estimate of  $CO_2$  conductance made in the unicellular green algae, *Dunaliella salina* (15). These conductances are calculated assuming that only  $CO_2$  is effluxing, rather than  $HCO_3^-$ . If  $HCO_3^-$  may also leave the cell via a reversal of the  $C_i$  transport system, then these values will be overestimates.

The simple model developed for  $C_i$  transport and photosynthesis, agrees remarkably with the actual measurements made on photosynthesizing cells. For a ratio of transport to fixation ( $V_i/V_c$ ) of less than 2, the model predicts that cell conductance to  $CO_2$  leakage would have to be less than  $10^{-4}$   $cm^2 s^{-1}$  (Fig. 2). For 30% leakage, this would be closer to  $10^{-5}$   $cm^2 s^{-1}$ . This is very close to the estimates of conductance from pool size and  $CO_2$  efflux measurements, assuming an internal pH of 8.0. The presence of CA is in agreement with the apparent necessity in the model, if total internal  $C_i$  is not to reach unmanageably high levels (Fig. 3). The measured values of internal activity sufficient to promote a 300-fold increase in interconversion rate, satisfy the requirements of the model, as this would lead to better than 90% equilibration between  $CO_2$  and  $HCO_3^-$  species. The lack of an effect of ethoxzolamide on  $C_i$  usage is inconsistent with measured CA activity, the model and previously reported effects on the cyanobacterium *A. variabilis* (7). The reason for this is not clear at present.

While the model based on  $HCO_3^-$  transport into the cell and  $CO_2$  efflux outward does fit the available experimental data, two features of both its predictions and the measurements from cells need some consideration. The prediction and measurement of apparently very low values for conductance to  $CO_2$  is very hard to explain in terms of the known properties of biological membranes and diffusion layers. This conductance is roughly equivalent to an unstirred water layer thickness of 1 cm and compares to total  $CO_2$  conductance values in leaves of  $10^{-1}$  to  $10^{-2}$   $cm^2 s^{-1}$ . Assuming that  $CO_2$  and  $O_2$  diffuse similarly in these cells, then these low conductances will pose severe problems to the escape of photosynthetically evolved  $O_2$ . Calculations show that at  $10^{-5}$   $cm^2 s^{-1}$ ,  $O_2$  would build up internally to levels between 2 and 7  $\mu M$  (Fig. 2). This is equivalent to partial pressures of 1.7 to 5.9 atmospheres of oxygen. This would certainly pose toxicity problems to the cell. Such a conductance would also pose problems to oxygen availability for respiration in the dark.

The resolution of the apparently low conductance values both in the model and experimental data, remain to be resolved; however, it is clear that the  $CO_2$  concentrating system in these cells operates relatively efficiently with leakage of  $CO_2$  not in excess of the  $C_4$  mechanism in higher plants. This would minimize the energy expenditure involved in concentrating  $CO_2$  at the site of carboxylation. Measured parameters of  $C_i$  fluxes in these cells can be simulated by the proposed simple  $HCO_3^-$  transport model. This, however, is not proof and resolution of the actual mechanism of  $CO_2$  concentration remains forthcoming.

### LITERATURE CITED

- BADGER MR 1980 Kinetic properties of  $RuP_2$  carboxylase from *Anabaena variabilis*. Arch Biochem Biophys 201: 247–254
- BADGER MR, TJ ANDREWS 1982 Photosynthesis and inorganic carbon usage by the marine cyanobacterium, *Synechococcus* sp. Plant Physiol 70: 517–523
- BERRY JA, J BOYNTON, A KAPLAN, MR BADGER 1976 Growth and photosynthesis of *Chlamydomonas reinhardtii* as a function of  $CO_2$  concentration. Carnegie Inst Wash Year Book 75: 423–432
- FARQUHAR GD 1983 On the nature of carbon isotope discrimination in  $C_4$  species. Aust J Plant Physiol 10: 205–226
- GUILLARD RRL, JH RYTHER 1962 Studies of marine planktonic diatoms. Can J Microbiol 8: 229–239
- INGLE RK, B COLMAN 1976 The relationship between carbonic anhydrase activity and glycolate excretion in the blue-green alga *Coccolithus elabens*: Responses to external  $CO_2$  concentration. Planta 149: 219–226
- KAPLAN A, MR BADGER, JA BERRY 1980 Photosynthesis and the intracellular inorganic carbon pool in the blue-green alga *Anabaena variabilis*: Responses

- to external CO<sub>2</sub> concentration. *Planta* 149: 219–226
8. KAPLAN A, D ZENVIRTH, L REINHOLD, JA BERRY 1982 Involvement of a primary electrogenic pump in the mechanism for HCO<sub>3</sub><sup>-</sup> uptake by the cyanobacterium *Anabaena variabilis*. *Plant Physiol* 69: 978–982
  9. MILLER AG, B COLMAN 1980 Active transport and accumulation of bicarbonate by a unicellular cyanobacterium. *J Bacteriol* 143: 1253–1259
  10. MILLER AG, B COLMAN 1980 A evidence for HCO<sub>3</sub><sup>-</sup> transport by the blue-green alga (Cyanobacterium) *Coccochloris peniocystis*. *Plant Physiol* 65: 397–402
  11. POCKER Y, DW BJORKQUIST 1977 Stopped-flow studies of carbon dioxide hydration and bicarbonate dehydration in H<sub>2</sub> and D<sub>2</sub>O. Acid-base and metal ion catalysis. *J Am Chem Soc* 99: 6537–6543
  12. RIPPKA R, J DERUELLES, JB WATERBURY, M HERDMAN, RY STAINER 1979 Generic assignments, strain histories, and properties of pure cultures of cyanobacteria. *J Gen Microbiol* 111: 1–61
  13. SILVERMAN DN 1974 A new approach to measuring the rate of rapid bicarbonate exchange across membranes. *Mol Pharmacol* 10: 820–836
  14. WINTERMANN JFGM, A DE MOTS 1965 Spectrophotometric characteristics of chlorophylls a and b and their pheophytins in ethanol. *Biochim Biophys Acta* 109: 448–453
  15. ZENVIRTH D, A KAPLAN 1981 Uptake and efflux of inorganic carbon in *Dunaliella salina*. *Planta* 152: 8–12